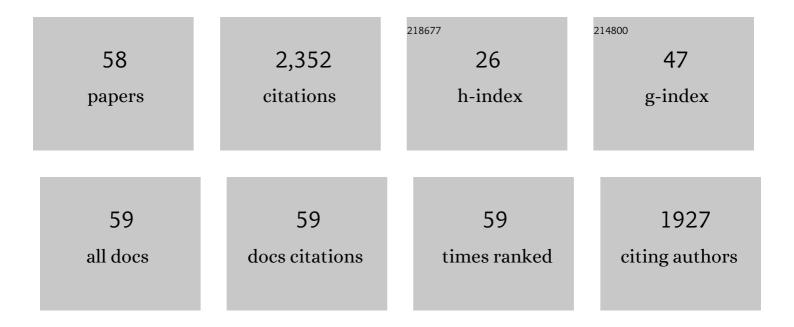
Jianping Long

List of Publications by Year in descending order

Source: https://exaly.com/author-pdf/1074809/publications.pdf Version: 2024-02-01



#	Article	IF	CITATIONS
1	An artificial hybrid interphase for an ultrahigh-rate and practical lithium metal anode. Energy and Environmental Science, 2021, 14, 4115-4124.	30.8	376
2	Understanding the Reaction Chemistry during Charging in Aprotic Lithium–Oxygen Batteries: Existing Problems and Solutions. Advanced Materials, 2019, 31, e1804587.	21.0	254
3	Heterostructured NiS ₂ /ZnIn ₂ S ₄ Realizing Toroid-like Li ₂ O ₂ Deposition in Lithium–Oxygen Batteries with Low-Donor-Number Solvents. ACS Nano, 2020, 14, 3490-3499.	14.6	113
4	Optimizing Redox Reactions in Aprotic Lithium–Sulfur Batteries. Advanced Energy Materials, 2020, 10, 2002180.	19.5	112
5	Interface engineering induced selenide lattice distortion boosting catalytic activity of heterogeneous CoSe2@NiSe2 for lithium-oxygen battery. Chemical Engineering Journal, 2020, 393, 124592.	12.7	84
6	Rationalizing the Effect of Oxygen Vacancy on Oxygen Electrocatalysis in Li–O ₂ Battery. Small, 2020, 16, e2001812.	10.0	81
7	In Situ Fabricating Oxygen Vacancy-Rich TiO ₂ Nanoparticles via Utilizing Thermodynamically Metastable Ti Atoms on Ti ₃ C ₂ Tx MXene Nanosheet Surface To Boost Electrocatalytic Activity for High-Performance Li–O ₂ Batteries. ACS Applied Materials &: Interfaces. 2019. 11. 46696-46704.	8.0	77
8	Design strategies toward catalytic materials and cathode structures for emerging Li–CO ₂ batteries. Journal of Materials Chemistry A, 2019, 7, 21605-21633.	10.3	75
9	Free-Standing Three-Dimensional CuCo ₂ S ₄ Nanosheet Array with High Catalytic Activity as an Efficient Oxygen Electrode for Lithium–Oxygen Batteries. ACS Applied Materials & Interfaces, 2019, 11, 3834-3842.	8.0	75
10	Highly reversible Li-O2 battery induced by modulating local electronic structure via synergistic interfacial interaction between ruthenium nanoparticles and hierarchically porous carbon. Nano Energy, 2019, 57, 166-175.	16.0	73
11	Three-Dimensional Interconnected Network Architecture with Homogeneously Dispersed Carbon Nanotubes and Layered MoS ₂ as a Highly Efficient Cathode Catalyst for Lithium–Oxygen Battery. ACS Applied Materials & Interfaces, 2018, 10, 34077-34086.	8.0	72
12	Tuning oxygen non-stoichiometric surface via defect engineering to promote the catalysis activity of Co3O4 in Li-O2 batteries. Chemical Engineering Journal, 2020, 381, 122678.	12.7	68
13	Interface-engineered metallic 1T-MoS2 nanosheet array induced via palladium doping enabling catalysis enhancement for lithium–oxygen battery. Chemical Engineering Journal, 2020, 382, 122854.	12.7	52
14	Morphology regulation of Li2O2 by flower-like ZnCo2S4 enabling high performance Li-O2 battery. Journal of Power Sources, 2019, 441, 227168.	7.8	49
15	Honeycomb-like Ni3S2 supported on Ni foam as high performance free-standing cathode for lithium oxygen batteries. Electrochimica Acta, 2018, 290, 657-665.	5.2	41
16	Phosphorus vacancies enriched Ni2P nanosheets as efficient electrocatalyst for high-performance Li–O2 batteries. Electrochimica Acta, 2020, 337, 135795.	5.2	39
17	Modulating electronic structure of honeycomb-like Ni2P/Ni12P5 heterostructure with phosphorus vacancies for highly efficient lithium-oxygen batteries. Chemical Engineering Journal, 2021, 413, 127404.	12.7	39
18	Heteroatom-Induced Electronic Structure Modulation of Vertically Oriented Oxygen Vacancy-Rich NiFe Layered Double Oxide Nanoflakes To Boost Bifunctional Catalytic Activity in Li–O ₂ Battery. ACS Applied Materials & Interfaces, 2019, 11, 29868-29878.	8.0	38

JIANPING LONG

#	Article	IF	CITATIONS
19	Componentâ€Interaction Reinforced Quasiâ€Solid Electrolyte with Multifunctionality for Flexible Li–O ₂ Battery with Superior Safety under Extreme Conditions. Small, 2019, 15, e1804701.	10.0	38
20	Tuning the electronic band structure of Mott–Schottky heterojunctions modified with surface sulfur vacancy achieves an oxygen electrode with high catalytic activity for lithium–oxygen batteries. Journal of Materials Chemistry A, 2020, 8, 11337-11345.	10.3	38
21	Three-dimensional CoNi2S4 nanorod arrays anchored on carbon textiles as an integrated cathode for high-rate and long-life Lithiumâ^'Oxygen battery. Electrochimica Acta, 2019, 301, 69-79.	5.2	34
22	Improved Cyclability of Lithium–Oxygen Batteries by Synergistic Catalytic Effects of Two-Dimensional MoS ₂ Nanosheets Anchored on Hollow Carbon Spheres. ACS Sustainable Chemistry and Engineering, 2019, 7, 6929-6938.	6.7	31
23	Anionic vacancy-dependent activity of the CoSe ₂ with a tunable interfacial electronic structure on the N-doped carbon cloth for advanced Li–O ₂ batteries. Journal of Materials Chemistry A, 2020, 8, 16636-16648.	10.3	31
24	Interlayer material technology of manganese phosphate toward and beyond electrochemical pseudocapacitance over energy storage application. Journal of Materials Science and Technology, 2021, 71, 109-128.	10.7	31
25	3D Array of Bi ₂ S ₃ Nanorods Supported on Ni Foam as a Highly Efficient Integrated Oxygen Electrode for the Lithiumâ€Oxygen Battery. Particle and Particle Systems Characterization, 2018, 35, 1700433.	2.3	30
26	A 3D free-standing Co doped Ni ₂ P nanowire oxygen electrode for stable and long-life lithium–oxygen batteries. Nanoscale, 2020, 12, 6785-6794.	5.6	30
27	Airflow Synergistic Needleless Electrospinning of Instant Noodleâ€like Curly Nanofibrous Membranes for Highâ€Efficiency Air Filtration. Small, 2022, 18, e2107250.	10.0	28
28	Threeâ€Dimensional Flowerâ€Like MoS ₂ @Carbon Nanotube Composites with Interconnected Porous Networks and High Catalytic Activity as Cathode for Lithiumâ€Oxygen Batteries. ChemElectroChem, 2018, 5, 2816-2824.	3.4	23
29	Configuration of gradient-porous ultrathin FeCo ₂ S ₄ nanosheets vertically aligned on Ni foam as a noncarbonaceous freestanding oxygen electrode for lithium–oxygen batteries. Nanoscale, 2020, 12, 1864-1874.	5.6	22
30	Multifunctional Selenium Vacancy Coupling with Interface Engineering Enables High-Stability Li–O ₂ Battery. ACS Sustainable Chemistry and Engineering, 2020, 8, 6667-6674.	6.7	22
31	Boosting pseudocapacitive energy storage performance via both phosphorus vacancy defect and charge injection technique over the CoP electrode. Journal of Alloys and Compounds, 2021, 864, 158106.	5.5	22
32	Two-dimensional spinel CuCo2S4 nanosheets as high efficiency cathode catalyst for lithium-oxygen batteries. Journal of Alloys and Compounds, 2019, 798, 560-567.	5.5	21
33	Cobalt encapsulated within porous MOF-derived nitrogen-doped carbon as an efficient bifunctional electrocatalyst for aprotic lithium-oxygen battery. Journal of Alloys and Compounds, 2019, 810, 151877.	5.5	20
34	Adjusting the d-band center of metallic sites in NiFe-based Bimetal-organic frameworks via tensile strain to achieve High-performance oxygen electrode catalysts for Lithium-oxygen batteries. Journal of Colloid and Interface Science, 2022, 607, 1215-1225.	9.4	20
35	Dendrite-Free Solid-State Li–O ₂ Batteries Enabled by Organic–Inorganic Interaction Reinforced Gel Polymer Electrolyte. ACS Sustainable Chemistry and Engineering, 2019, 7, 17362-17371.	6.7	19
36	Excellent electrolyte-electrode interface stability enabled by inhibition of anion mobility in hybrid gel polymer electrolyte based Li–O2 batteries. Journal of Membrane Science, 2020, 604, 118051.	8.2	19

JIANPING LONG

#	Article	IF	CITATIONS
37	Defect regulation of heterogeneous nickel-based oxides via interfacial engineering for long-life lithium-oxygen batteries. Electrochimica Acta, 2019, 321, 134716.	5.2	16
38	Invigorating the Catalytic Activity of Cobalt Selenide via Structural Phase Transition Engineering for Lithium–Oxygen Batteries. ACS Sustainable Chemistry and Engineering, 2020, 8, 5018-5027.	6.7	16
39	Effect of replacement of Ca by Zn on the structure and optical property of CaTiO ₃ :Eu ³⁺ red phosphor prepared by solâ€gel method. Luminescence, 2015, 30, 533-537.	2.9	15
40	NiCo ₂ S ₄ Nanorod Arrays Supported on Carbon Textile as a Free‣tanding Electrode for Stable and Longâ€Life Lithiumâ€Oxygen Batteries. ChemElectroChem, 2019, 6, 349-358.	3.4	15
41	Interfacial electronic structure design of MXene-based electrocatalyst via vacancy modulation for lithium-oxygen battery. Carbon, 2020, 166, 273-283.	10.3	11
42	Synergy of cobalt vacancies and iron doping in cobalt selenide to promote oxygen electrode reactions in lithium-oxygen batteries. Journal of Colloid and Interface Science, 2022, 612, 171-180.	9.4	11
43	Promoting the Electrocatalytic Activity of Ti ₃ C ₂ T _x MXene by Modulating CO ₂ Adsorption through Oxygen Vacancies for Highâ€Performance Lithiumâ€Carbon Dioxide Batteries. ChemElectroChem, 2020, 7, 4922-4930.	3.4	10
44	Theoretical Investigation of the Newly Noncentrosymmetric Superconductor SrAuSi3 via First Principles. Journal of Superconductivity and Novel Magnetism, 2015, 28, 3235-3241.	1.8	8
45	3D porous network gel polymer electrolyte with high transference number for dendrite-free Li O2 batteries. Solid State Ionics, 2019, 343, 115088.	2.7	8
46	A multifunctional protective layer with biomimetic ionic channel suppressing dendrite and side reactions on zinc metal anodes. Journal of Colloid and Interface Science, 2022, 613, 136-145.	9.4	8
47	Luminescence enhancement of (Sr _{1–<i>x</i>} M _{<i>x</i>}) ₂ SiO ₄ :Eu ² ⁺ phosphors with M (Ca ² ⁺ /Zn ² ⁺) partial substitution for white lightâ€emitting diodes. Luminescence, 2017, 32, 119-124.	supz 2.9	7
48	Tuning the Unsaturated Coordination Center of Electrocatalysts toward High-Performance Lithium–Oxygen Batteries. ACS Sustainable Chemistry and Engineering, 2021, 9, 7499-7507.	6.7	6
49	First-principles calculations of structural phase transition and elastic properties of BeTe under high pressure. Philosophical Magazine Letters, 2014, 94, 103-111.	1.2	5
50	Modulating in-plane electron density of molybdenum diselenide via spontaneously atomic-scale palladium doping enables high performance lithium oxygen batteries. Journal of Alloys and Compounds, 2021, 855, 157484.	5.5	5
51	Luminescence Enhancement of ZnS:Cu Nanocrystals by Zinc Sulfide Coating with Core/Shell Structure. Integrated Ferroelectrics, 2014, 154, 110-119.	0.7	3
52	Al2O3/TiO2 core/shell powder derived by novel sol–gel routes. Journal of Sol-Gel Science and Technology, 2015, 75, 475-480.	2.4	3
53	Synthesis and photoluminescence of Eu ³⁺ /Dy ³⁺ -doped CaGdAlO ₄ phosphors for white light emitting diodes. Integrated Ferroelectrics, 2017, 179, 148-158.	0.7	3
54	Electrochemical Kinetics of Layered Manganese Phosphate via Interfacial Polypyrrole Chemical Binding. ChemElectroChem, 0, , .	3.4	3

#	Article	IF	CITATIONS
55	Sol–gel synthesis and luminescence property of Sr ₄ Al ₂ O ₇ :Re3 ⁺ ,R ⁺ (ReÂ=ÂEu and Dy; RÂ=ÂLi,	Na)2.Tg ETÇ	<u>9</u> q111 0.784 <mark>31</mark>
56	Active site synergy of the mixed-phase cobalt diselenides with slight lattice distortion for highly reversible and stable lithium oxygen batteries. Journal of Materials Science and Technology, 2021, 92, 159-170.	10.7	1
57	Preparation and modification of polythiophene-organic montmorillonite composite. Polymer Composites, 2016, 37, 2503-2510.	4.6	ο
58	Promoted redox chemistry of high sulfur content cathode via endowing fast Li-ion diffusion. Ionics, 2022, 28, 1473-1481.	2.4	0